Title
Fermi LARGE AREA TELESCOPE OBSERVATIONS OF BLAZAR 3C 279 OCCULTATIONS BY THE SUN

Journal
The Astrophysical Journal, 784(2)

ISSN
0004-637X

Authors
Barbiellini, G
Bastieri, D
Bechtol, K
et al.

Publication Date
2014-04-01

DOI
10.1088/0004-637x/784/2/118

Peer reviewed

Published in final edited form as:
Astrophys J. 2014 April 01; 784(2): . doi:10.1088/0004-637X/784/2/118.

Fermi LARGE AREA TELESCOPE OBSERVATIONS OF BLAZAR 3C 279 OCCULTATIONS BY THE SUN

A full list of authors and affiliations appears at the end of the article.

Abstract

Observations of occultations of bright γ-ray sources by the Sun may reveal predicted pair halos around blazars and/or new physics, such as, e.g., hypothetical light dark matter particles—axions. We use *Fermi Gamma-Ray Space Telescope* (*Fermi*) data to analyze four occultations of blazar 3C 279 by the Sun on October 8 each year from 2008 to 2011. A combined analysis of the observations of these occultations allows a point-like source at the position of 3C 279 to be detected with significance of $\approx 3\sigma$, but does not reveal any significant excess over the flux expected from the quiescent Sun. The likelihood ratio test rules out complete transparency of the Sun to the blazar γ-ray emission at a 3σ confidence level.

Keywords

astroparticle physics; gamma rays: general; occultations; quasars: individual (3C 279); Sun: X-rays, gamma rays

1. INTRODUCTION

Blazar 3C 279 is the brightest extragalactic source that is occulted by the Sun. The first observation of the solar occultation of 3C 279 in γ-rays was reported by Fairbairn et al. (2007) using the EGRET data from 1991, who found an excess of $\delta F(>100\,\mathrm{MeV}) = \left(6.2^{+3.7}_{-2.7}\right) \times 10^{-7}$ photons cm^{-2} s^{-1}. This observation has led to a speculation (Fairbairn et al. 2007, 2010) about the possible detection of a pair halo around the blazar or an axion-like particle.

The possible existence of extended, diffuse, γ-ray sources (so-called pair halos) around blazars was predicted by Aharonian et al. (1994). γ-rays with energies above ~1 TeV cannot propagate over cosmological distances because of the production of $e^{\pm}$-pairs on the diffuse extragalactic background light. In turn, the $e^{\pm}$ pairs emit secondary cascade γ-rays owing to inverse Compton (IC) scattering by cosmic microwave background photons. Therefore, a γ-ray image of an active galactic nucleus (AGN) is expected to exhibit a halo of secondary photons around a bright central point-like source. Either a detection or a non-detection of pair halos could put important limits on the intergalactic magnetic field (Neronov & Vovk 2010). Pair halos have not been detected yet (Neronov et al. 2011; Ackermann et al. 2013).

imos@stanford.edu, phdmitry@stanford.edu.

An axion is a hypothetical light particle that is an attractive dark matter candidate. Axions were introduced to solve the strong CP problem in QCD (for a recent review see Kim & Carosi 2010). A possible coupling of the photon and pseudoscalar (axion-like) field suggests that a photon has a finite probability to convert to an axion-like particle in the presence of an external magnetic field, and vice versa (Sikivie 1983; Raffelt & Stodolsky 1988). Note that axion-like particles are a more general class of particles whose mass and coupling are unrelated to each other whereas mass and coupling are related for axions.

Axion detection experiments (Kim & Carosi 2010) use many different techniques also used for detection of weakly interacting massive particles, but some are unique for axions, e.g., microwave receiver detectors, axion helioscopes, and experiments utilizing laser photons traversing a magnetic field. The latter experiments search for a polarization shift of the laser beam, dubbed “light shining through walls,” and magneto-optical vacuum effects. The modern “light shining through walls” experiments use optical photons emitted by a laser and 1–10 m size magnets with $B \approx 5$–10 T. The third generation axion helioscope CAST, which uses a prototype Large Hadron Collider magnet with $B = 9$ T to track the Sun for 3 hr a day, is currently operating at CERN. It looks for the flux of axions with an average energy of ~4.2 keV at the Earth produced in the core of the Sun by the Primakoff conversion of thermal photons in the Coulomb fields of nuclei and electrons. The current limit on axion–photon–photon coupling from CAST is $<8.8 \times 10^{-11}$ GeV^{-1} for axion mass $m_a \lesssim$ 0.02 eV (Andriamonje et al. 2007). Although, this upper limit is quite tight, there are some theoretical models which can reconcile the upper limit from CAST with the transparency of the Sun to γ-rays (see Fairbairn et al. 2007, and references therein).

The solar occultation experiment could provide a complementary probe of axion physics. This setup is similar to the laser “light shining through walls” experiment, but uses more energetic γ-ray photons from a blazar together with the magnetic field of the Sun. Observations of the occultations of bright γ-ray sources by the Sun can provide a unique opportunity to test the conversion of photons to axion-like particles during their passage through the strong and extended magnetic field of the upper layers of the Sun. The axions can then convert back into photons. An increased flux from the Sun during such an occultation would provide evidence of new physics (Fairbairn et al. 2007).

Meanwhile, the analysis by Fairbairn et al. (2007) was made under an assumption that the quiescent Sun does not emit γ-rays and was based on a non-detection of the Sun by the EGRET. The latter yielded only the upper limit of 2.0×10^{-7} photons cm^{-2} s^{-1} for the emission from the solar disk (Thompson et al. 1997).

However, the Sun is a bright extended γ-ray source. The emission from the solar disk due to the cosmic-ray cascades in the solar atmosphere was predicted by Seckel et al. (1991). The extended emission around the Sun due to the IC scattering of cosmic-ray electrons off solar photons was predicted by Moskalenko et al. (2006) and Orlando & Strong (2007). The intensity of both components of the solar emission changes with a period of ~11 yr due to the heliospheric modulation affecting the flux of Galactic cosmic rays. The reanalysis of the EGRET data (Orlando & Strong 2008) indeed revealed two components of the emission, $F_{\rm d}(>100\ {\rm MeV}) = (1.8 \pm 1.1) \times 10^{-7}$ photons cm^{-2} s^{-1} for the disk and $F_{\rm IC}$ (>100 MeV)

= $(3.8 \pm 2.1) \times 10^{-7}$ photons cm^{-2} s^{-1} for the extended component from a region of 10° radius centered on the Sun. An analysis of the first 18 months of data from the *Fermi* Large Area Telescope (LAT), launched in 2008, allows for a clear separation of the two components of the solar emission and yields their spectra as well as the angular profile of the extended component (Abdo et al. 2011). The observed integral fluxes were found to be $F_{\rm d}(>100\,{\rm MeV}) = \left(4.6 \pm 0.2[{\rm stat.}]^{+1.0}_{-0.8}[{\rm syst.}]\right) \times 10^{-7}$ photons cm^{-2} s^{-1} for the solar disk, and $F_{\rm IC}(>100\,{\rm MeV}) = \left(6.8 \pm 0.7[{\rm stat.}]^{+0.5}_{-0.4}[{\rm syst.}]\right) \times 10^{-7}$ photons cm^{-2} s^{-1} for the extended emission from a region of 20° radius centered on the Sun.

The launch of *Fermi* enabled monitoring of the quiescent Sun with high statistical significance and on a daily basis. Since occultations of 3C 279 last only ~8.5 hr, this capability of the *Fermi*-LAT is of critical importance. It provides us with an excellent opportunity to check the results of EGRET observations of the solar occultation of 3C 279.

The goal of this paper is to search for a signature of new physics through the establishment of flux in excess of what is expected from the quiescent Sun and a demonstration of the analysis method, rather than setting up limits on the axion parameter space or intergalactic magnetic field. The latter would require a significant increase in the event statistics. In this paper, we report on the analysis of the *Fermi*-LAT observations of four solar occultations of 3C 279 on October 8 each year from 2008 to 2011.

2. *Fermi*-LAT OBSERVATIONS OF 3C 279 OCCULTATIONS

2.1. Observation and Data Reduction

Fermi was launched on 2008 June 11 into nearly circular Earth orbit with an altitude of 565 km, an inclination of $25\overset{\circ}{.}6$, and an orbital period of 96 minutes. The principal instrument on *Fermi* is the LAT (Atwood et al. 2009), a pair-production telescope with a large effective area (~8000 cm^{-2} at 1 GeV) and field of view (2.4 sr) sensitive to γ-rays between 20 MeV and >300 GeV. After the commissioning phase, the *Fermi*-LAT began routine science operations on 2008 August 4. The *Fermi*-LAT normally operates in sky-survey mode where the whole sky is observed every 3 hr (i.e., two orbits).

For the data analysis, we use the *Fermi* Science Tools v9r27p1 package[51] and P7V6 instrument response functions. Events ⩾100 MeV arriving within 20° of 3C 279 (region of interest—ROI) and satisfying the SOURCE event selection are selected. The systematic uncertainty of the effective area for the SOURCE class events is estimated as 10% at 100 MeV, decreasing to 5% at 560 MeV, and increasing to 10% at 10 GeV and above. To reduce the contamination by the γ-ray emission from the Earth's limb, we select events with zenith angles <100°.

Besides 3C 279, there are eight other strong γ-ray sources listed in the 2FGL *Fermi*-LAT source catalog (Nolan et al. 2012) with integral fluxes in excess of 5.0×10^{-8} photons cm^{-2} s^{-1} above 100 MeV in the ROI along with the Sun that passes through this region from

[51] http://fermi.gsfc.nasa.gov/ssc/data/analysis/

September 17 to October 28 each year. The three brightest sources listed in the 2FGL are blazar 3C 273, quasar PKS 1329−049, and an unassociated source, 2FGL J1231.2−1411, at $(\mathrm{RA},\ \mathrm{decl.}) = (187.^{\circ}81,\ -14.^{\circ}18)$ for the epoch J2000.

The occultations of 3C 279 occur on October 8 each year. The beginning and end times of each solar occultation are calculated using the IDL astronomy library[52] which gives the solar position in J2000 epoch celestial coordinates. The occultation of 3C 279 starts when the separation between the solar center and the blazar becomes smaller than the solar disk radius of $\simeq 0.^{\circ}266$ (the angular radius corresponding to the occultation date) and lasts for ≈8 hr 34 minutes. We also took into account the parallax due to the orbital motion of *Fermi* by taking the entry times to be 4 minutes later and the exit times 4 minutes earlier than the nominal times. There were four occultations observed by *Fermi*-LAT in 2008–2011.

2.2. Likelihood Analysis and Results

We adopt a background model for the ROI that includes components describing the diffuse Galactic and isotropic γ-ray emission.[53] The Galactic diffuse component was held fixed, while the normalization of the isotropic component was allowed to vary. The spatially extended solar emission from the IC scattering of solar photons by cosmic-ray electrons (Moskalenko et al. 2006; Orlando & Strong 2007) was fixed using the best-fit map derived from the analysis of the *Fermi*-LAT observations (Abdo et al. 2011).

The periods of occultations of 3C 279 were analyzed using the unbinned maximum likelihood mode of *gtlike*, which is part of the Science Tools. The test statistic (TS; Mattox et al. 1996) was employed to evaluate the significance of the γ-ray fluxes coming from the source located at the position of 3C 279 during the occultations. The TS value is defined as twice the difference between the log-likelihood function, maximized by adjusting all the parameters of the model, with and without the source, and under the assumption of a precise knowledge of the Galactic and isotropic diffuse emission.

The normalization of the isotropic component in the ROI was evaluated using the data from the first three years of the *Fermi* mission, excluding time intervals when the Sun was in the ROI. We used this normalization in the subsequent analysis of the point sources.

Along with the Sun, the model includes eight bright 2FGL sources in the ROI. Their spectral shapes were taken from the 2FGL catalog (Nolan et al. 2012), while normalizations for the three brightest sources and the Sun were derived from the likelihood analysis. The spectral index of 3C 279, 2.22 ± 0.02, in the 2FGL catalog is fairly close to that of the solar disk, 2.11 ± 0.73 (Abdo et al. 2011). Therefore, 3C 279 and the Sun were considered as a single source (with the spectral index corresponding to that of 3C 279 and a free normalization) when the angular distance between them is $\lesssim 1^{\circ}$. The TS values for a point-like source at the position of 3C 279 for each of the four occultations were found to be ≲4, which correspond to the source significance of $\lesssim 2\sigma$.

[52] http://idlastro.gsfc.nasa.gov/ftp/pro/astro/, routines sunpos.pro and precess.pro
[53] The LAT standard diffuse emission models (gal_2yearp7v6_v0.fits and iso_p7v6source.txt), available at http://fermi.gsfc.nasa.gov/ssc/data/access/lat/BackgroundModels.html

Even though the TS for each occultation is relatively small, the solar path is clearly seen in Figure 1, which shows the residual count map with background counts subtracted, corresponding to the passage of the Sun through the ROI between 2008 September 17 and October 28. The background was taken from observations of the same region during 10 months following 2008 October 28. The total number of background counts in the ROI was then normalized to the total number of counts, corresponding to observations between 2008 September 17 and October 28. The residual map was smoothed with a two-dimensional Gaussian kernel of $\sigma = 1.^{\circ}5$. The positions of the 2FGL sources, with integral fluxes in excess of 5.0×10^{-8} photons cm^{-2} s^{-1} above 100 MeV, are marked with circles. The apparent oversubtraction at the position of 3C 279 is due to the flaring activity of the blazar during the months following 2008 October 28.[54] The figure shows that the Sun is clearly detectable on a timescale of days.

The error in the determination of the source flux is dominated by the statistical error due to the short observational time intervals, ~8.5 hr for each occultation, and, correspondingly, limited photon statistics. In contrast, the statistical and systematic errors associated with the evaluation of the Galactic and isotropic backgrounds are considerably smaller due to the much larger photon count collected over three years of the *Fermi* mission. Hereafter, we show only statistical error bars deduced from the fit to the Sun plus bright sources in the ROI.

To increase the significance of the signal from the point-like source at the position of 3C 279 during the occultations, we perform a stacking analysis of the four occultations using the python module *SummedLikelihood* from the *Fermi* Science Tools that statistically "sums" likelihood objects. The combined analysis yields a TS value of 8.7. Therefore, the point-like source at the position of 3C 279 is detected with significance of $\approx 3\sigma$. The corresponding integral flux is $(2.7 \pm 1.3) \times 10^{-7}$ photons cm^{-2} s^{-1} above 100 MeV. This flux can be compared with the integral flux from the solar disk, $F_d(>100\ \mathrm{MeV}) = (4.6 \pm 1.0) \times 10^{-7}$ photons cm^{-2} s^{-1}, derived from the analysis of observations of the quiescent Sun (Abdo et al. 2011). Assuming that the solar disk flux was the same during the occultations of 3C 279 in 2008–2011, these observations do not yield any excess relative to the emission of the solar disk.

2.3. γ-Ray Emission from 3C 279

The amplitude of the possible effect of "shining light through a wall," owing to the presence of axion-like particles, should be proportional to the photon flux from 3C 279, and, therefore, the result of Section 2.2 would be incomplete without an evaluation of the blazar flux during the occultation. A reasonable proxy for that is an average of the emission from 3C 279 just before and immediately after the occultations.

To estimate the fluxes from 3C 279 during the occultations, we analyze the blazar flux a day before and a day after each occultation. To increase statistics, we stack the intervals before and after each occultation using a module of *SummedLikelihood*. Since the exposures

[54] http://fermi.gsfc.nasa.gov/ssc/data/access/lat/msl_lc/source/3C_279

of the survey-mode observations of the occultations differ significantly for different years, we take this into account by scaling the exposures of the blazar observations accordingly. The longest exposure corresponds to the occultation in 2011. We, therefore, choose the longest time interval before and after the occultation in 2011 equal to 24 hr corresponding to the exposure ~8.5×10^7 cm^2 s and scale exposures in other years proportionally to the occultation exposures, i.e., 0.93:0.34:0.41:1.0, for 2008, 2009, 2010, and 2011 correspondingly.

Since the maximum separation between the solar disk center and 3C 279 is less than ~$1\overset{\circ}{.}25$ during these time intervals, considerably smaller than the *Fermi*-LAT point-spread function (PSF) ≃6° at 100 MeV, we interpret this flux as the sum of the fluxes from the solar disk and 3C 279. We perform the unbinned likelihood analysis for data taken within specified time intervals around the occultation time, taking into account the Galactic, isotropic, and solar IC diffuse sources as well as 3C 279, and the eight other strong sources from the 2FGL catalog. The procedure of the likelihood analysis is the same as described in Section 2.2.

The derived fluxes and statistical uncertainties are shown in Table 1. A comparison of the fluxes before and after each occultation shows their consistency within the statistical uncertainties. Note that there was an episode of a strong flaring activity of 3C 279 on 2010 September 27–28, about ten days before the occultation. It is, therefore, possible that the 3C 279 luminosity was changing during the occultation on a short timescale, which may be reflected in a difference between fluxes before and after the occultation (Table 1). The combined analysis yields TS value 230 and, therefore, the source at the position of 3C 279 is detected with significance of $\approx 15\sigma$. The exposure-weighted flux value is $(7.5 \pm 0.8) \times 10^{-7}$ photons cm^{-2} s^{-1} and is significantly higher than that obtained from the analysis of the four occultations.

To compare several models of the observed occultations, we use the likelihood ratio test. The following three models were chosen as “null” models: (1) the absence of the source at the position of 3C 279, (2) the source with the flux of $\approx 4.6 \times 10^{-7}$ photons cm^{-2} s^{-1}, corresponding to the solar disk flux (Abdo et al. 2011), and (3) complete transparency of the solar disk to γ-ray photons of 3C 279. The latter corresponds to a source at the position of 3C 279 with flux of $\approx 7.5 \times 10^{-7}$ photons cm^{-2} s^{-1}. The alternative model assumes a source at the position of 3C 279 with a free flux normalization, which gives the flux $(2.7 \pm 1.3) \times 10^{-7}$ photons cm^{-2} s^{-1} above 100 MeV as described above.

The likelihood analysis described in Section 2.2 gives the TS value 8.7 for a comparison of the 1st null and alternative models, 1.6 for the 2nd null and alternative models, and 9.1 for the 3rd null and alternative models. The first TS value corresponds to the case that was already considered above. Since each of the three null models represents a special case of the alternative model, the probability distribution of the TS is approximately a chi-square distribution with one degree of freedom—the difference between the numbers of free parameters of the null and alternative models. Therefore, the 1st model, with no source, and the 3rd model, which assumes a complete transparency of the solar disk, can be ruled out with the confidence level of 3σ. Instead, the 2nd model with the source flux, corresponding to that of the solar disk, agrees with the alternative model within 1.5σ. Note

that the solar disk flux used in the 2nd model was taken from the analysis of the first 18 months of the *Fermi*-LAT mission (Abdo et al. 2011) corresponding to the solar minimum. Since the solar disk flux is expected to decrease during the period of increased solar activity, the emission from the solar disk taken over a longer time interval should be weaker than that measured in 2008–2009 and would provide a better description of the data.

3. OUTLOOK

In this section, we compare different techniques for the pair halo search and discuss constraints on the coupling constant between photons and axions that can be obtained from the solar occultation experiment.

3.1. Pair Halo Search for 3C 279

A pair halo is a putative extended γ-ray source around an AGN (Aharonian et al. 1994). Pair halos have not been detected yet; the *Fermi*-LAT Collaboration reported only an upper limit (Ackermann et al. 2013) so far based on the stacked analysis of low- and high-redshift BL Lac AGN and the TeV blazars.

Fairbairn et al. (2010) proposed a method to search for emission from a pair halo by using the solar disk to screen out the direct emission from a bright AGN. In order for this method to provide a lower background for searches the solar disk must be less bright than the AGN. However, the Sun itself is a bright γ-ray source (Abdo et al. 2011); consequently for 3C 279 a more sensitive search for a pair halo can be made by studying time intervals when the source is in a low state.

In the presented analysis of 3C 279 during its low flux state, we use the binned likelihood analysis. We consider a region of 30° radius centered at 3C 279 (the ROI). All of the 2FGL sources were included in the model. Besides 3C 279, the sources with a free normalization for fitting include 2FGL J1313.0−0425, 2FGL J1229.1+0202, 2FGL J1231.2−1411, 2FGL J1239.5+0443, 2FGL J1332.0−0508, 2FGL J1246.7−2546, 2FGL J1126.6−1856, 2FGL J1224.9+2122, 2FGL J1311.7−3429, and Galactic and isotropic templates.

The spectral–spatial model includes a putative pair halo source. The latter is modeled as an extended disk source with a radius of $1.^{\circ}5$ at 500 MeV, where the radius is scaled with energy as $1/E$ (see, e.g., Neronov & Semikoz 2009). Taking into account the energy-dependent angular size of a pair halo source and the *Fermi*-LAT PSF, we select the energy range for this analysis from 500 MeV–100 GeV with 23 logarithmic energy bins. Although, there is a significant uncertainty in models predicting the angular size of the pair halos around a blazar, the angular radius of $1.^{\circ}5$ at ~500 MeV is a reasonable assumption. This also allows for a clear discrimination from a point source given the *Fermi*-LAT angular resolution.

We analyzed the light curve of 3C 279 to search for time intervals when the flux from the blazar was low compared to that from the solar disk as reported in Abdo et al. (2011). The analysis shows that the blazar flux was low between 2012 March 14 and 2013 April 18. The *Fermi*-LAT observations during this time interval result in upper limits on the blazar flux for the most of the week-long intervals analyzed. For time intervals when 3C 279 was detected,

the average flux in the low-flux state was $F(E > 500\ \mathrm{MeV}) = (1.6 \pm 0.1) \times 10^{-8}$ photons $\mathrm{cm}^{-2}\ \mathrm{s}^{-1}$.

Performing likelihood analysis for week-long intervals (as in Section 2.2), we compare the models including a point source and a disk source (without a point source) at the position of 3C 279. The interval is 58 weeks between 2012 March 14 and 2013 April 18. The spectral parameters of the sources in the ROI correspond to those in the 2FGL catalog. The normalization of the flux is a free parameter in both analyses. The model involving a point source provides a higher likelihood value and the difference of the log-likelihood values is $d \ln L = 34.5$. Thus, the relative likelihood of the model with a disk source, with respect to the model with a point source, is $\exp(-d \ln L) \simeq 1 \times 10^{-15}$.

Using the model that includes both the point and disk sources at the position of 3C 279, we computed the one-sided 95% confidence level upper limit on the pair halo flux. We found that the upper limit equals $3.3{\times}10^{-9}$ photons $\mathrm{cm}^{-2}\ \mathrm{s}^{-1}$ for energies greater than 500 MeV. This value is significantly lower than that obtained from the interpolation of the flux observed during the occultations, $F(E > 500\ \mathrm{MeV}) = 5.4{\times}10^{-8}$ photons $\mathrm{cm}^{-2}\ \mathrm{s}^{-1}$.

Since the calculated 95% flux upper limit is lower than that obtained from the interpolation of the flux observed during the four occultations, we conclude that the method of studying the pair halo around 3C 279 based on observations of low flux blazar states is preferred over the method that uses the four occultations that happened during the solar minimum conditions. The solar minimum conditions correspond to higher fluxes of Galactic protons and electrons and thus the emission from proton cascades in the solar atmosphere and from IC scattering of CR electrons off solar photons is correspondingly brighter.

3.2. Axion–Photon Coupling

We re-examine the constraints on the coupling constant between photons and axions, g, as a function of axion mass, m_{a}, that can be obtained from the solar occultation experiment. Note that there are two limitations on the results of the solar occultation experiment. The first comes from the setup of this experiment and is determined by the strength of solar magnetic fields, the plasma density, and the size of the photon–axion conversion region. This limitation is unavoidable and is discussed in the Appendix. The second is due to the sensitivity of the detector and is determined by the number of counts in the direction of the Sun detected during occultations of 3C 279.

To calculate the probability of observing a fraction of photon flux from 3C 279 that has passed through the Sun, one needs to make an assumption on the photon–axion ratio for the beam entering the Sun. Following Fairbairn et al. (2007), we assume that the beam incident from the blazar has a photon⁄axion ratio of 2:1. Since only photons polarized parallel to the magnetic field mix with axions, and the three-dimensional magnetic field configuration is inhomogeneous, an efficient photon–axion conversion would cause an average depletion of 66% of the initial photon beam (see, e.g., Mirizzi et al. 2008). To derive the constraints on the coupling constant from the solar occultation experiment (see the Appendix), the statistical error on the observed photon flux should be significantly smaller than 33% of the initial photon flux from 3C 279. The statistical error on the photon flux observed during the

four occultations is $\Delta F_{\rm stat} = 1.3 \times 10^{-7}$ photons cm^{-2} s^{-1} and is significantly smaller than the summed exposure-weighted flux, $(7.5 \pm 0.8) \times 10^{-7}$ photons cm^{-2} s^{-1}, from the Sun and 3C 279 measured just before and after the occultations. One third of the average flux for the four intervals considered together is 2.5×10^{-7} photons cm^{-2} s^{-1} and is larger than the statistical error $\Delta F_{\rm stat}$. However, the contribution from the Sun (Abdo et al. 2011) to the summed flux is significant, $\simeq 4.6 \times 10^{-7}$ photons cm^{-2} s^{-1}, and this does not allow us to constrain the coupling constant yet.

An analysis of the daily light curve of 3C 279 during the first five years of the *Fermi*-LAT mission shows that the blazar flux at $E > 100$ MeV exceeds 10^{-6} photons cm^{-2} s^{-1} on approximately 10% of the days. We performed 1000 simulations of a pointed observation of a solar occultation of 3C 279 (about 8.5 hr each) assuming the Sun to have the solar flux reported by Abdo et al. (2011). By means of the likelihood analysis of each simulated data set and applying the optimization algorithm NEWMINUIT, we found that the average statistical error of the measurement is $\simeq 1.7 \times 10^{-7}$ photons cm^{-2} s^{-1} and is less than one third of the blazar flux at its high state. Therefore, the pointed observation of the Sun during an occultation of 3C 279 when the blazar flux is high should constrain the coupling constant.

4. DISCUSSION AND CONCLUSION

We found that 13 point-like γ-ray sources from the 2FGL catalog (Nolan et al. 2012) are occulted by the Sun, which include 3C 279, PKS 1437 153, EGR J1800–2328, LAT PSR J1809–2332, PKS 2335−027, GB6 J0708+2241, TXS 0723+220, BZB J0912+1555 and unassociated sources 2FGL J0923.5+1508, 2FGL J1624.2−2124, 2FGL J1727.8−2308, 2FGL J2031.4−1842, 2FGL J2124.0−1513. Blazar 3C 279 is the strongest source in this list, except EGR J1800–2328 and LAT PSR J1809–2332, which are projected onto the Galactic plane. Since the background emission from the Galactic plane is significantly higher than that at high latitudes, 3C 279 ($b = +57°$) is best suited for observations of occultations.

A stacking analysis of the *Fermi*-LAT observations during the occultations in 2008, 2009, 2010, and 2011 allows us to detect a point-like source at the position of 3C 279 with flux of $(2.7 \pm 1.3) \times 10^{-7}$ photons cm^{-2} s^{-1} above 100 MeV and significance of $\simeq 3\sigma$. This flux is consistent within the 1σ uncertainties with the flux of the solar disk $F_{\rm d}(>100\ {\rm MeV}) = (4.6 \pm 1.0) \times 10^{-7}$ photons cm^{-2} s^{-1}, thus providing no evidence of excess emission.

A stacking analysis of observations during the intervals before and after each occultation yields the exposure-weighted flux of $(7.5 \pm 0.8) \times 10^{-7}$ photons cm^{-2} s^{-1}. This flux was interpreted as the sum of the fluxes from the solar disk and 3C 279. A likelihood ratio test rules out a complete transparency of the solar disk at the confidence level of 3σ. This is the first direct evidence of the opacity of the solar disk to γ-rays from 3C 279.

Using the reanalysis of the EGRET data by Orlando & Strong (2008), it is possible to rectify the results by Fairbairn et al. (2007). The reanalysis of the EGRET data for a period from 1991 October (near the solar maximum) to 1995 June (close to the solar minimum) yielded the integral flux from the solar disk of $F_{\rm d}(>100\ {\rm MeV}) = (1.8 \pm 1.1) \times 10^{-7}$ photons cm^{-2} s^{-1}. Using this flux one can estimate the emission excess found for the occultation

of 3C 279 in 1991. We found that the corrected excess flux during the occultation is $\delta F(>100\,\mathrm{MeV}) = \left(4.4^{+4.8}_{-3.8}\right)\times 10^{-7}$ photons cm^{-2} s^{-1}, which is only ~1σ significance. This result is consistent with our analysis of the *Fermi*-LAT data.

The main motivation of the analysis described in this paper is a search for new physics, not necessarily axions or pair halos. It demonstrates the feasibility of the technique that can be used for the analysis of solar occultations in the future, but the statistics collected at present do not yet allow for the detailed interpretation of the result beyond a simple statement that the observed flux is consistent, within the 1σ uncertainties, with the flux of the solar disk. The combined exposure of the survey-mode observations of the four blazar occultations is $\approx 32 \times 10^6$ cm^2 s, which is nearly equivalent to a single pointed observation of the occultations of 3C 279 by *Fermi*. If the occulted blazar is in high state and the Sun is in low state (corresponding to the solar cycle maximum), a single pointed observation of the occultation would be enough to put tighter constraints on the opacity of the solar disk to γ-rays from 3C 279.

Authors

G. Barbiellini[1,2], D. Bastieri[3,4], K. Bechtol[5], R. Bellazzini[6], R. D. Blandford[5], A. W. Borgland[5], J. Bregeon[6], P. Bruel[7], R. Buehler[5], S. Buson[3,4], G. A. Caliandro[8], R. A. Cameron[5], P. A. Caraveo[9], E. Cavazzuti[10], C. Cecchi[11,12], R. C. G. Chaves[13], A. Chekhtman[14,48], C. C. Cheung[15,49], J. Chiang[5], S. Ciprini[10,12], R. Claus[5], J. Cohen-Tanugi[16], F. D'Ammando[11,17,18], A. de Angelis[19], C. D. Dermer[20], S. W. Digel[5], E. do Couto e Silva[5], P. S. Drell[5], A. Drlica-Wagner[5], C. Favuzzi[21,22], W. B. Focke[5], A. Franckowiak[5], Y. Fukazawa[23], P. Fusco[21,22], F. Gargano[22], D. Gasparrini[10], S. Germani[11,12], N. Giglietto[21,22], P. Giommi[10], F. Giordano[21,22], M. Giroletti[24], T. Glanzman[5], G. Godfrey[5], I. A. Grenier[13], J. E. Grove[20], S. Guiriec[25], D. Hadasch[8], M. Hayashida[5,26], E. Hays[25], R. E. Hughes[27], M. S. Jackson[28,29], T. Jogler[5], J. Knödlseder[30,31], M. Kuss[6], J. Lande[5], S. Larsson[29,32,33], F. Longo[1,2], F. Loparco[21,22], M. N. Lovellette[20], P. Lubrano[11,12], M. N. Mazziotta[22], J. Mehault[17], P. F. Michelson[5], T. Mizuno[34], A. A. Moiseev[35,36], C. Monte[21,22], M. E. Monzani[5], A. Morselli[37], I. V. Moskalenko[5], S. Murgia[5], R. Nemmen[25], E. Nuss[16], T. Ohsugi[34], N. Omodei[5], M. Orienti[24], E. Orlando[5], D. Paneque[5,38], J. S. Perkins[25,35,39,40], F. Piron[16], G. Pivato[4], D. Prokhorov[5,49], S. Rainò[21,22], M. Razzano[6,41,42], S. Razzaque[14], A. Reimer[5,43], O. Reimer[5,43], S. Ritz[41,42], C. Romoli[4], M. Sánchez-Conde[5], D.A. Sanchez[44], C. Sgrò[6], E. J. Siskind[45], G. Spandre[6], P. Spinelli[21,22], H. Takahashi[23], T. Tanaka[5], L. Tibaldo[3,4], M. Tinivella[6], G. Tosti[11,12], E. Troja[25,50], T. L. Usher[5], J. Vandenbroucke[5], V. Vasileiou[16], G. Vianello[5,46], V. Vitale[37,47], A. P. Waite[5], B. L. Winer[27], K. S. Wood[20], Z. Yang[29,30]

Affiliations

[1]Istituto Nazionale di Fisica Nucleare, Sezione di Trieste, I-34127 Trieste, Italy

[2]Dipartimento di Fisica, Università di Trieste, I-34127 Trieste, Italy

[3]Istituto Nazionale di Fisica Nucleare, Sezione di Padova, I-35131 Padova, Italy

[4]Dipartimento di Fisica e Astronomia “G. Galilei,” Università di Padova, I-35131 Padova, Italy

[5]W. W. Hansen Experimental Physics Laboratory, Kavli Institute for Particle Astrophysics and Cosmology, Department of Physics and SLAC National Accelerator Laboratory, Stanford University, Stanford, CA 94305, USA;

[6]Istituto Nazionale di Fisica Nucleare, Sezione di Pisa, I-56127 Pisa, Italy

[7]Laboratoire Leprince-Ringuet, École polytechnique, CNRS/IN2P3, Palaiseau, France

[8]Institut de Ciències de l’Espai (IEEE-CSIC), Campus UAB, E-08193 Barcelona, Spain

[9]INAF-Istituto di Astrofisica Spaziale e Fisica Cosmica, I-20133 Milano, Italy

[10]Agenzia Spaziale Italiana (ASI) Science Data Center, I-00044 Frascati (Roma), Italy

[11]Istituto Nazionale di Fisica Nucleare, Sezione di Perugia, I-06123 Perugia, Italy

[12]Dipartimento di Fisica, Università degli Studi di Perugia, I-06123 Perugia, Italy

[13]Laboratoire AIM, CEA-IRFU/CNRS/Université Paris Diderot, Service d’Astrophysique, CEA Saclay, F-91191 Gif sur Yvette, France

[14]Center for Earth Observing and Space Research, College of Science, George Mason University, Fairfax, VA 22030, USA

[15]National Research Council Research Associate, National Academy of Sciences, Washington, DC 20001, USA

[16]Laboratoire Univers et Particules de Montpellier, Université Montpellier 2, CNRS/IN2P3, Montpellier, France

[17]IASF Palermo, 90146 Palermo, Italy

[18]INAF-Istituto di Astrofisica Spaziale e Fisica Cosmica, I-00133 Roma, Italy

[19]Dipartimento di Fisica, Università di Udine and Istituto Nazionale di Fisica Nucleare, Sezione di Trieste, Gruppo Collegato di Udine, I-33100 Udine, Italy

[20]Space Science Division, Naval Research Laboratory, Washington, DC 20375-5352, USA

[21]Dipartimento di Fisica “M. Merlin” dell’Università e del Politecnico di Bari, I-70126 Bari, Italy

[22]Istituto Nazionale di Fisica Nucleare, Sezione di Bari, I-70126 Bari, Italy

[23]Department of Physical Sciences, Hiroshima University, Higashi-Hiroshima, Hiroshima 739-8526, Japan

[24]INAF Istituto di Radioastronomia, I-40129 Bologna, Italy

[25]NASA Goddard Space Flight Center, Greenbelt, MD 20771, USA

[26]Department of Astronomy, Graduate School of Science, Kyoto University, Sakyo-ku, Kyoto 606-8502, Japan

[27]Department of Physics, Center for Cosmology and Astro-Particle Physics, The Ohio State University, Columbus, OH 43210, USA

[28]Department of Physics, Royal Institute of Technology (KTH), AlbaNova, SE-106 91 Stockholm, Sweden

[29]The Oskar Klein Centre for Cosmoparticle Physics, AlbaNova, SE-106 91 Stockholm, Sweden

[30]CNRS, IRAP, F-31028 Toulouse cedex 4, France

[31]GAHEC, Université de Toulouse, UPS-OMP, IRAP, Toulouse, France

[32]Department of Physics, Stockholm University, AlbaNova, SE-106 91 Stockholm, Sweden

[33]Department of Astronomy, Stockholm University, SE-106 91 Stockholm, Sweden

[34]Hiroshima Astrophysical Science Center, Hiroshima University, Higashi-Hiroshima, Hiroshima 739-8526, Japan

[35]Center for Research and Exploration in Space Science and Technology (CRESST) and NASA Goddard Space Flight Center, Greenbelt, MD 20771, USA

[36]Department of Physics and Department of Astronomy, University of Maryland, College Park, MD 20742, USA

[37]Istituto Nazionale di Fisica Nucleare, Sezione di Roma “Tor Vergata,” I-00133 Roma, Italy

[38]Max-Planck-Institut für Physik, D-80805 München, Germany

[39]Department of Physics and Center for Space Sciences and Technology, University of Maryland Baltimore County, Baltimore, MD 21250, USA

[40]Harvard-Smithsonian Center for Astrophysics, Cambridge, MA 02138, USA

[41]Department of Physics, Santa Cruz Institute for Particle Physics, University of California at Santa Cruz, Santa Cruz, CA 95064, USA

[42]Department of Astronomy and Astrophysics, Santa Cruz Institute for Particle Physics, University of California at Santa Cruz, Santa Cruz, CA 95064, USA

[43]Institut für Astro-und Teilchenphysik and Institut für Theoretische Physik, Leopold-Franzens-Universität Innsbruck, A-6020 Innsbruck, Austria

[44]Max-Planck-Institut für Kernphysik, D-69029 Heidelberg, Germany

[45]NYCB Real-Time Computing Inc., Lattingtown, NY 11560-1025, USA

[46]Consorzio Interuniversitario per la Fisica Spaziale (CIFS), I-10133 Torino, Italy

[47]Dipartimento di Fisica, Università di Roma “Tor Vergata,” I-00133 Roma, Italy

[48]Resident at Naval Research Laboratory, Washington, DC 20375, USA.

[49]Current address: Max-Planck-Institut für Astrophysik, D-85741 München, Germany.

[50]NASA Postdoctoral Program Fellow, USA.

Acknowledgments

The *Fermi*-LAT Collaboration acknowledges generous ongoing support from a number of agencies and institutes that have supported both the development and the operation of the LAT as well as scientific data analysis. These include the National Aeronautics and Space Administration and the Department of Energy in the United States; the Commissariat à l'Energie Atomique and the Centre National de la Recherche Scientifique/Institut National de Physique Nucléaire et de Physique des Particules in France; the Agenzia Spaziale Italiana and the Istituto Nazionale di Fisica Nucleare in Italy; the Ministry of Education, Culture, Sports, Science and Technology (MEXT), High Energy Accelerator Research Organization (KEK), and Japan Aerospace Exploration Agency (JAXA) in Japan; and the K. A. Wallenberg Foundation, the Swedish Research Council, and the Swedish National Space Board in Sweden.

Additional support for science analysis during the operations phase is gratefully acknowledged from the Istituto Nazionale di Astrofisica in Italy and the Centre National d'Études Spatiales in France. I.V.M. acknowledges support from NASA grant NNX12AO73G.

APPENDIX

The Lagrangian density for axions coupling to a magnetic field is given by (for a review, see Mirizzi et al. 2008):

$$\mathscr{L} = -\frac{1}{4} g F_{\mu\nu} \tilde{F}^{\mu\upsilon} a = g \boldsymbol{E} \boldsymbol{B} a, \tag{A1}$$

where a is the axion field, F is the electromagnetic field-strength, $\tilde{F}$ is its dual, $\boldsymbol{E}$ is the electric field, $\boldsymbol{B}$ is the magnetic field, and g is the axion–photon coupling with dimensions of inverse energy. The mixing term, $F_{\mu\nu}\tilde{F}^{\mu\nu}a$, involves two photons, one of them corresponding to an external field. Henceforth, we use the Lorentz–Heaviside (LH) system of units with $\hbar = c = 1$ and a fine structure constant $\alpha = e^2/4\pi = 1/137$.

The probability of axion–photon conversion was derived by Raffelt & Stodolsky (1988) and Anselm & Uraltsev (1982). We use its parameterization given in Gnedin et al. (2007) and Hooper & Serpico (2007):

$$P(\gamma_{\parallel} \leftrightarrow a) = \frac{1}{1+x^2} \sin^2\left(\frac{1}{2} B g L \sqrt{1+x^2}\right), \tag{A2}$$

where $x = (\epsilon - 1)\omega/2Bg$, ω is the photon frequency, ϵ is the dielectric function of the solar medium where the light is propagating, B is the magnetic field component perpendicular to the photon direction, and L is the size of the conversion region.

For the dielectric function of the medium, one can write:

$$\epsilon - 1 = \frac{m_{\mathrm{a}}^2 - \omega_{\mathrm{pl}}^2}{\omega^2}, \tag{A3}$$

where $\omega_{\rm pl} = \sqrt{4\pi\alpha n_{\rm e}/m_{\rm e}}$ is the effective plasma frequency, n_e is the total electron number density including both free and bound electrons, and m_e is the electron rest mass. γ-rays interact with free and bound electrons resulting in an increase of the effective plasma frequency. Here, we neglected the contribution of polarizability of vacuum, which is important only for very strong magnetic fields such as near a neutron star or a magnetic white dwarf.

As can be seen from Equation (A2), the mixing between photons and axions is maximal when the parameter $x=\left(m_{\rm a}^2-\omega_{\rm pl}^2\right)/2\omega Bg$ is small. This condition is fulfilled when the photon frequency, ω, is high or when the conversion takes place in the resonant region with $\omega_{\rm pl} \approx m_{\rm a}$ (e.g., Fairbairn et al. 2007). An appreciable, significant conversion also requires that the argument of the oscillatory function in Equation (A2) is not small, i.e., $(1/2)BgL \gtrsim 1$. These two cases, when the conversion probability is high, could be expressed as:

1. non-resonant

$$\begin{aligned} m_{\rm a}^2/(2\omega Bg) &\lesssim 1 \\ \omega_{\rm pl}^2/(2\omega Bg) &\lesssim 1 \\ \frac{1}{2}BgL &\gtrsim 1 \end{aligned} \tag{A4}$$

2. resonant

$$\begin{aligned} \left(m_{\rm a}^2-\omega_{\rm pl}^2\right)/(2\omega Bg) &\lesssim 1 \\ \frac{1}{2}BgL &\gtrsim 1. \end{aligned} \tag{A5}$$

Therefore, the conditions for the non-resonant case are fulfilled when $g \gtrsim \max\left\{m_{\rm a}^2/(2\omega B), \omega_{\rm pl}^2/(2\omega B), 2/(BL)\right\}$.

It is useful to introduce the dimensionless quantities: $B_{\rm G} = B/{\rm Gauss}$, $L_{\rm Mm} = L/{\rm Mm}$, $m_{\rm meV} = m_a/{\rm meV}$, and $n_{15} = n_{\rm e}/(10^{15}\ {\rm cm}^{-3})$, where the scales are typical for the solar occultation experiment.[55] Note that in the LH units, 1 G = 0.069 eV^2, and 1 cm = 5.07×10^4 eV^{-1}. Thus, the system Equation (A4) can be rewritten as (ω = 100 MeV):

$$\begin{aligned} g &\gtrsim 7.2\times10^{-14}\left(m_{\rm meV}^2/B_{\rm G}\right){\rm eV}^{-1} \\ g &\gtrsim 1.0\times10^{-13}(n_{15}/B_{\rm G}){\rm eV}^{-1} \\ g &\gtrsim 5.7\times10^{-12}(B_{\rm G}L_{\rm Mm})^{-1}{\rm eV}^{-1}, \end{aligned} \tag{A6}$$

see also Fairbairn et al. (2007). For the resonant case, only the last inequality in the system Equation (A6) is required. Note that the limit on the coupling constant is inversely

[55] We assume that the conversion of photons to axion-like particles and vice versa takes place in the upper layers where the absorption of γ-rays can be neglected.

proportional to the magnetic field strength and, therefore, the region of higher magnetic field strength, ≃100 G, provides better constraints.

At sufficiently low values of the axion–photon coupling, which still allow photons to be efficiently converted to axions in the upper layers of the Sun, the effects associated with the passage of axions through the inner layers of the Sun, such as the conversion of axions to photons (with immediate absorption of photons) and the decrease in the axion flux, are small (see Fairbairn et al. 2007).

REFERENCES

Abdo AA, Ackermann M, Ajello M, et al. 2011, ApJ, 734, 116
Ackermann M, Ajello M, Allafort A, et al. 2013, ApJ, 765, 54
Aharonian FA, Coppi PS, & Voelk HJ 1994, ApJL, 423, L5
Andriamonje S, Aune S, Autiero D, et al. 2007, JCAP, 04, 010
Anselm AA, & Uraltsev NG 1982, PhLB, 116, 161
Atwood WB, Abdo AA, Ackermann M, et al. 2009, ApJ, 697, 1071
Fairbairn M, Rashba T, & Troitsky S 2007, PhRvL, 98, 201801
Fairbairn M, Rashba T, & Troitsky S 2010, MNRAS, 403, L6
Gnedin YN, Piotrovich MY, & Natsvlishvili TM 2007, MNRAS, 374, 276
Hooper D, & Serpico PD 2007, PhRvL, 99, 231102
Kim JE, & Carosi G 2010, RvMP, 82, 557
Mattox JR, Bertsch DL, Chiang J, et al. 1996, ApJ, 461, 396
Mirizzi A, Raffelt GG, & Serpico PD 2008, in Lecture Notes in Physics, Axions, Vol. 741, ed. Kuster M, Raffelt G, & Beltrán B (Berlin: Springer), 115
Moskalenko IV, Porter TA, & Digel SW 2006, ApJL, 652, L65
Neronov A, & Semikoz DV 2009, PhRvD, 80, 123012
Neronov A, Semikoz DV, Tinyakov PG, & Tkachev II 2011, A&A, 526, A90
Neronov A, & Vovk I 2010, Sci, 328, 73
Nolan PL, Abdo AA, Ackermann M, et al. 2012, ApJS, 199, 31
Orlando E, & Strong AW 2007, Ap&SS, 309, 359
Orlando E, & Strong AW 2008, A&A, 480, 847
Raffelt G, & Stodolsky L 1988, PhRvD, 37, 1237
Seckel D, Stanev T, & Gaisser TK 1991, ApJ, 382, 652
Sikivie P 1983, PhRvL, 51, 1415
Thompson DJ, Bertsch DL, Morris DJ, & Mukherjee R 1997, JGR, 102, 14735

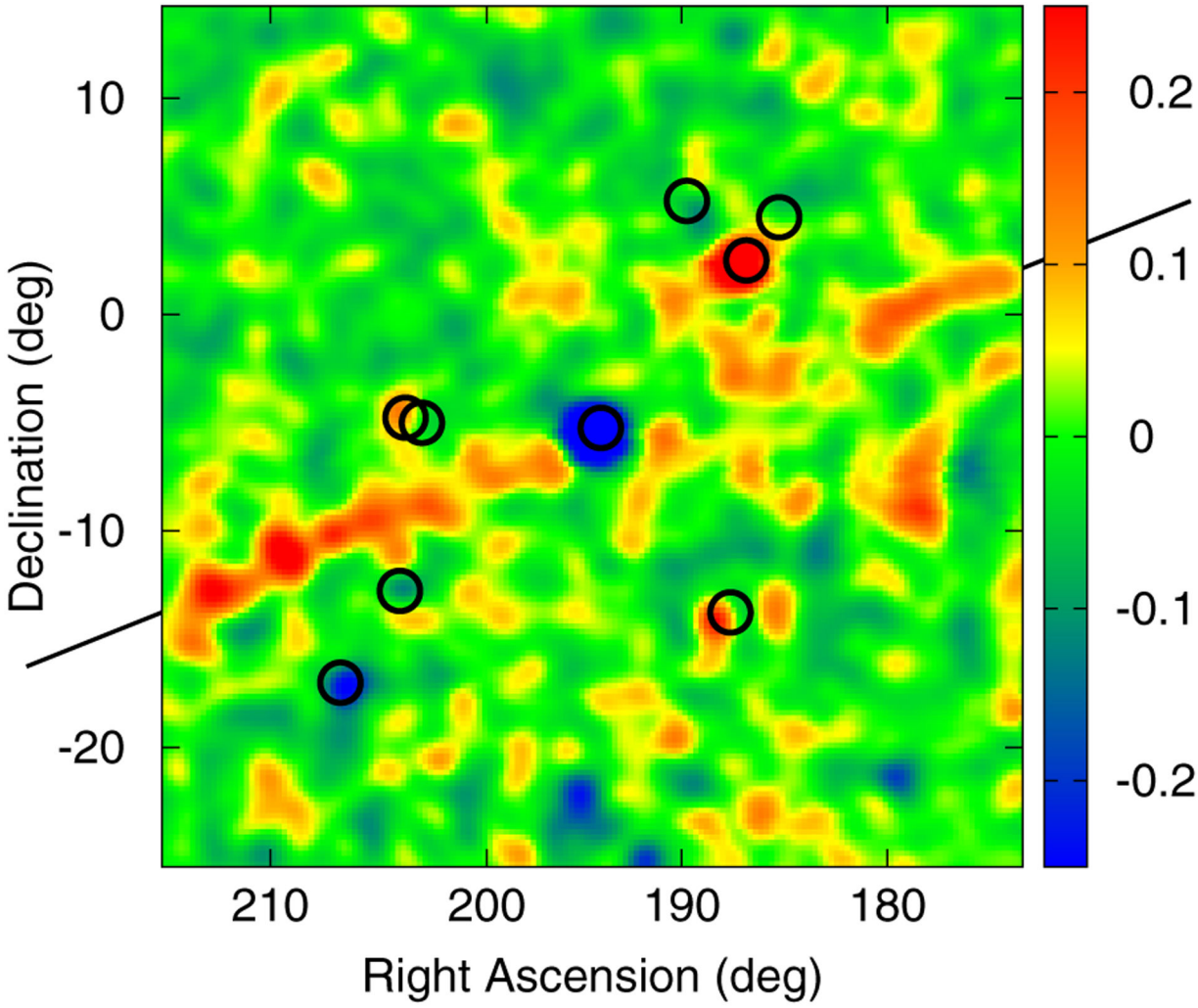

Figure 1.

Solar track (the solid line is added for guidance) is clearly seen in the residual map (>1 GeV) and corresponds to observations between 2008 September 17 and October 28. The color bar shows counts per pixel, pixel size is $0.^{\circ}25 \times 0.^{\circ}25$. The central position of the map corresponds to the position of 3C 279 (oversubtracted). Positions of bright sources are shown with circles.

Table 1

The Combined Flux of 3C 279 and the Sun Before and After the Occultation

	Flux (>100 MeV), 10^{-7} photons cm^{-2} s^{-1}	
Year	**Before**	**After**
2008	7.5 ± 2.0	6.7 ± 2.0
2009	10.5 ± 3.6	9.8 ± 3.5
2010	12.1 ± 3.5	6.3 ± 3.0
2011	7.5 ± 1.9	4.5 ± 1.7
2008–2011	Combined: 7.5 ± 0.8	